ACS APPLIED ENGINEERING MATERIALS

pubs.acs.org/acsaenm

Article

Water-Repellent Spray for Textiles Using Plant Waste from Conifer Trees

Sara K. Fleetwood, Sydney Bell, Reinhard Jetter, and E. Johan Foster*

Cite This: ACS Appl. Eng. Mater. 2024, 2, 1288−1297

Read Online

ACCESS | Metrics & More | Article Recommendations | Supporting Information

ABSTRACT: A superhydrophobic textile coating, applied by using a home drying machine, was developed as an aqueous dispersion of waxes that were extracted from recycled Christmas trees. Because the bulk extraction of waxes yielded a mixture of hydrophobic and hydrophilic compounds, a purification process was tested to determine if removing noncrystallizing wax components would enhance the performance of the coating. The performances of coatings created from the crude and enriched extracts were compared, and no significant difference in hydrophobicity was found. Moreover, although the enriched coating was slightly more breathable, there was not enough of an improvement to justify the additional purification steps, rendering the crude extract more industrially viable. Overall, Christmas tree waxes are readily sourced and are capable of producing superhydrophobic coatings without the need for a costly purification step.

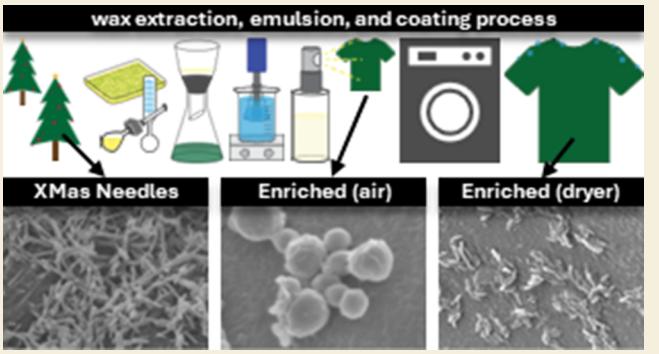

KEYWORDS: *hydrophobic, coating, plant-based, plant waste, plant wax, Abies procera*

1. INTRODUCTION

Hydrophobic coatings (water contact angle (WCA) > 90°) are used in a wide range of applications from automotive to food packaging, totaling a $2.2 billion dollar industry.[1] Among these industries, textile applications make up 11.1% and include furniture, clothing (e.g., cotton and polyester shirts, rain jackets, and leather shoes), carpets, tents, and tarps.[2] Worldwide, 73.1% of the commercially available hydrophobic coatings, or durable water-repellent (DWR) coatings, contain fluoropolymers and fluoroalkylsilanes due to their thermal stability, low surface energy, and chemical inertness.[1] However, perfluorinated compounds (PFCs) are considered environmentally persistent and toxic, leading regulatory bodies, including the Environmental Protection Agency, to phase out PFCs with carbon chain lengths of eight or more.[2]

While the number of commercially available PFC-free coatings is on the rise, these are generally petroleum-based, limiting their potential applications when sustainability is of concern.[3] To improve the coating's hydrophobicity without the use of PFCs, researchers have also begun looking for nanoparticles to emulate the lotus effect, which combines a hierarchical surface roughness with a high surface energy to achieve a superhydrophobic surface (WCA > 150°).[4] When these two properties are present, air pockets form at the solid−liquid interface that are too small for water to penetrate, suspending the water droplets on the surface of the air and substrate (Cassie−Baxter state).[5,6] A common example is the incorporation of engineered nanoparticles into low-surface-energy coatings to increase surface roughness and achieve superhydrophobicity. However, Som et al. showed that nanoparticles (e.g., ZnO, SiO_2) may impact human health (e.g., toxicity, brain damage, respiratory tract) and the environment (e.g., stability during incineration, indication of hazardous effects, toxic effects from dissolution in water).[7] To counteract some of the health hazards of existing hydrophobic coatings, the overarching goal of the current work was to produce aqueous wax dispersions that are petroleum- and PFC-free, with no emulsifiers used to stabilize the dispersions.

Within the literature, researchers have investigated biobased coating alternatives, such as carnauba wax.[6,8−10] While plant waxes are generally composed of a mixture of ubiquitous long-chain aliphatic compounds, commercially available plant wax coatings are typically amorphous in physical structure, with low surface-to-volume ratios, limiting their hydrophobicity.[11] Alternatively, some plant species produce "specialty compounds" that can assemble into crystal shapes that afford high contact angles—for example, the majority of the wax of the sacred lotus (the species for which the "lotus effect" is named) is nonacosan-10-ol and nonacosanediols, which self-assemble

Received: February 20, 2024
Revised: April 25, 2024
Accepted: April 29, 2024
Published: May 9, 2024

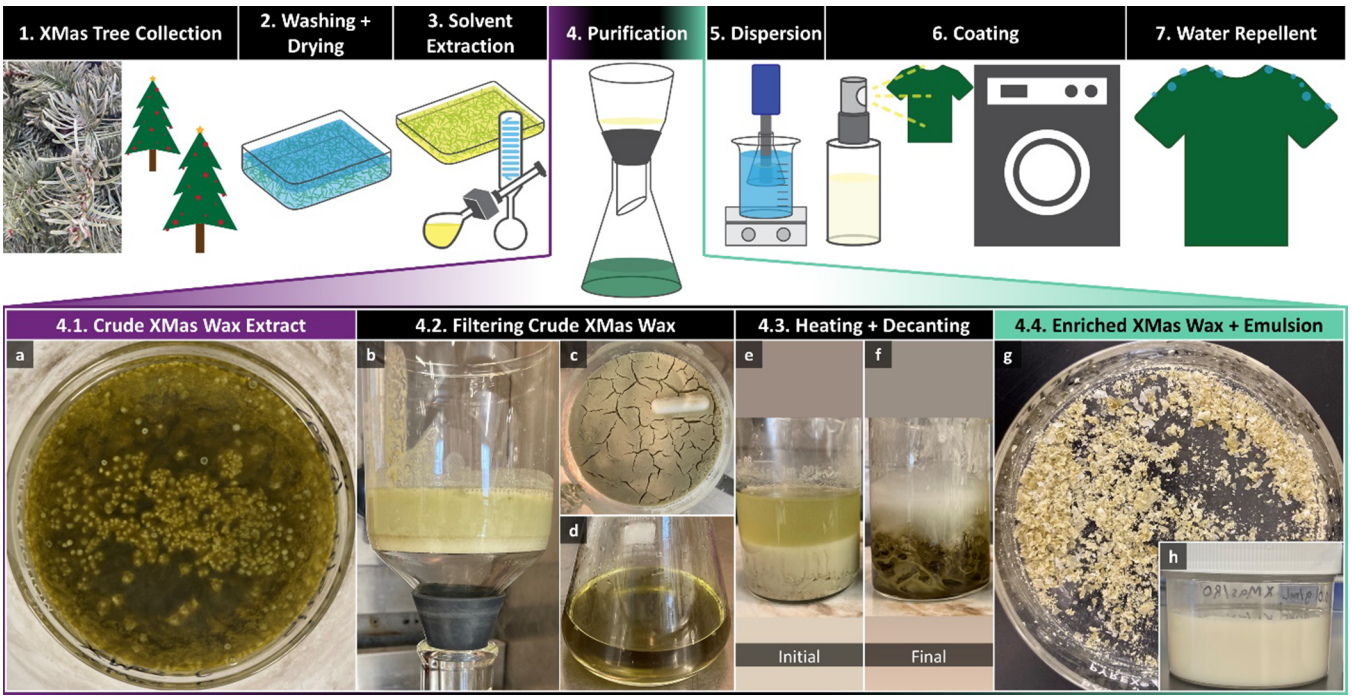

Figure 1. Christmas (XMas) tree wax isolation process and preparation of the hydrophobic coating for application to textiles. The top row illustrates the overall process: (1) branches from XMas tree recycling programs were cut and dried in cotton bags. Needles were removed (2) and washed with water. (3) Waxes covering the needles were extracted with chloroform, and the resulting solutions were concentrated using a rotary evaporator. Either the crude wax or parts of it resulting from (4) partial purification were (5) dispersed in water at concentrations of 0.01 g/mL. (6) The dispersions were sprayed onto textiles and dried at room temperature or with mild heating (in a home drying machine), (7) resulting in a water-repellent textile. The bottom row illustrates the partial purification of the wax mixture: (4.1) the crude wax mixture seen (a) top-down separated into two layers based on polarity. To remove the hydrophilic extract, (4.2) the crude wax mixture was washed first with methanol at room temperature and then with (4.3) hot methanol. First, the (a) crude wax was (b) filtered with methanol into the (c) residue and (d) filtrate. Then, the (e–f) residue was redispersed in methanol, heated, and decanted into solute and precipitate. (4.4) (g) Purified wax came from the residue-solute, from which a (h) dispersion was prepared.

into nanotubules.[11] This process is driven by the favorable burial of the midchain hydroxyl groups while positioning the compounds' methyl groups on the surface, thus increasing the surface's nanoroughness and subsequently its water repellency.[4] Therefore, we investigated the use of nonacosan-10-ol as it has the potential of yielding a superhydrophobic coating and is not currently commercially available large-scale.

In our prior work, we demonstrated a proof of concept, developing a superhydrophobic water-repellent spray for coating textiles using nonacosan-10-ol wax extracted from the seasonal leaf litter of ginkgo trees.[12] To improve upon this, we aimed to source the waxes from an underutilized industrial waste stream, subsequently adding value to that plant source. In our previous work, we screened the amount, composition, and waterproofing performance of waxes among six plant species. Of these, we found the conifer had the highest amount of nonacosan-10-ol by surface area, and the resulting coating achieved superhydrophobicity.[12] Furthermore, studies suggest that many other conifer species also contain large quantities of nonacosan-10-ol[13] on their needles. We therefore focused on industries that produce specific conifer waste, selecting the Christmas (XMas) tree industry. XMas trees are often recycled into low-value products, such as mulch, after the holiday season. Locally, the noble fir (*Abies procera* Rehder) accounts for 45% of XMas trees grown in the Pacific Northwest (PNW), which supplies one-third of the 36 million XMas trees sold within the US.[14] Furthermore, a majority of XMas trees grown globally are fir trees, which are commonly known to contain nonacosan-10-ol.[15] Thus, the XMas tree industry represents a large supply of nonacosan-10-ol that is otherwise lost after trees are recycled into low-value byproducts.[14]

In the current work, we investigate the performance of XMas tree waxes as a hydrophobic coating for textiles (cotton and polyester shirts) that is applied as an aqueous dispersion and recrystallized using a home drying machine.[12] Additionally, given the abundance of oleoresins and terpenes typically found in conifer extracts, we aimed to increase the relative quantity of nonacosan-10-ol (an enriched extract) to compare it to the crude extract. In order to obtain an enriched extract, we used a modified version of the method of isolating nonacosan-10-ol from spruce extracts by McElroy et al., in which they use three successive separations: the first and third in room-temperature methanol, via recrystallization, and the second in hot methanol, via decanting.[16] The primary differences from our previous work include: (1) shifting the wax source from deciduous leaf litter to coniferous industrial waste and (2) comparing the coating performance of a crude extract against an enriched extract, as we anticipated that the enriched extract would yield a more hydrophobic and breathable coating.[12] The following techniques were used to characterize the wax extract and coating: differential scanning calorimetry (DSC), dynamic light scattering (DLS), water contact angle (WCA), scanning electron microscopy (SEM), water vapor permeance (WVP), gas chromatography–mass spectrometry (GC–MS), and a gas chromatography-flame ionization detector (GC–FID).

https://doi.org/10.1021/acsaenm.4c00116
ACS Appl. Eng. Mater. 2024, 2, 1288–1297

2. EXPERIMENTAL SECTION

2.1. Materials

Branches of XMas trees, mostly comprising noble fir (*Abies procera*), were harvested from The University of British Columbia's (UBC) botanical garden (Vancouver, Canada) tree recycling program. Chloroform (CAS 67-66-3), methanol (CAS 67-56-1), primuline (CAS 8064-60-6), pyridine (CAS 110-86-1), and *N*,*O*-bis-(trimethylsilyl)trifluoroacetamide (BSTFA) (CAS 25561-30-2) were purchased from Sigma-Aldrich (St. Louis, United States of America).

The commercial spray-on coating, referred to as "CommCoat" throughout the remainder of the article, was purchased directly from the manufacturer. CommCoat is marketed for use on technical outerwear fabrics, is petroleum-based, and contains PFCs.

Two different substrates, with hydrophobic or hydrophilic surfaces, were used for testing the coatings. 100% polyester knit (039400 Scuba, 008 off white) and 100% cotton twill (0900801 Cotton Twill, 006 greige) were purchased from Fabricland Online (Toronto, Canada). First, all of the fabrics were washed using the seventh-generation laundry detergent (Fresh Lavender Scent) and subsequently dried. The rain jacket fabric (referred to as "Rain Jacket" throughout the remainder of the article) is a trilaminate containing nylon plain weave face fabric (80 deniers), expanded polytetrafluoroethylene membrane (ePTFE), and polyester backer, with a PFC-free DWR.

2.2. Plant Wax Isolation and Coating Processes from Conifer Sources

2.2.1. Wax Extraction. Branches were cut from Christmas trees after the holidays in January. To separate needles from branches, branches were dried in cotton bags under ambient conditions until their moisture content was below 10%. In some cases, the bags with needles were placed in a fume hood to increase airflow, decreasing the drying time from approximately 1 month to a few days. Needles were then harvested from the branches by shaking and, in some cases, by manually pulling.

The needles were washed with water (Figure 1, top row), and the wax was extracted following a procedure similar to the large-scale wax isolation of Fleetwood et al.[12] Here, batches of ca. 200 g needles were extracted using chloroform in a 254 × 381 mm rectangular glass dish. Chloroform was removed through rotary evaporation, the concentrated extract was transferred to a Pyrex Petri dish, and residual chloroform was removed in the fume hood by evaporating. The resulting crude wax was stored at room temperature for further use.

2.2.2. Wax Purification To Enrich in Nonacosan-10-ol. To remove hydrophilic compounds, the protocol developed by McElroy et al. was modified[16] to perform extraction steps with methanol at room temperature and at elevated temperature (Figure 1, bottom row). For the room temperature extraction, a 300 mL beaker was charged with approximately 100 g of crude wax, 100 mL of methanol, and a small magnetic stir bar. This beaker was placed on a hot plate, externally set at 100 °C, and stirred at 1000 rpm for 15 min, after which the solution was left to cool to room temperature. The slurry was then vacuum-filtered through a funnel with a fritted disc (40−90 μm nominal maximal pore size) and washed with methanol (3 × 10 mL) at room temperature. The filtrate was then poured into a Pyrex Petri dish.

For the hot extraction, the residue was scraped off the fritted disc and placed into a 100 mL beaker, to which additional methanol was added to reach 50 mL. The beaker was heated on a hot plate externally set at 150 °C for 15 min. The temperature was then lowered to 120 °C for approximately 5 min or until the dispersion appeared to be stable. The supernatant was then decanted into a Pyrex Petri dish, and the remaining slurry was poured into a separate Pyrex Petri dish.

All samples, poured into Pyrex Petri dishes, were left in the fume hood until the remaining solvent evaporated. Samples were then stored under ambient conditions for further use. This process yielded three final products: residue-solute, residue-precipitate, and filtrate. A single batch of crude wax was processed.

2.2.3. Suspension for Hydrophobic Spray. Dispersions of the different wax mixtures were prepared following the procedure by Fleetwood et al.[12] In summary, 0.01 g/mL wax-RO (reverse osmosis) water dispersions were homogenized for 30 min at 15,000 rpm using an IKA T25 Ultra-Turrax Homogenizer (Staufen, Germany), mounted with an S25 N-18G Dispersing Tool (Figure 1.5). Then, the dispersions were each quenched and vacuum-filtered.

2.2.4. Coating Textiles by Spraying. Textiles were coated with 0.01 g/mL wax dispersions following a procedure similar to Fleetwood et al.[12] The dispersions were poured into Dynalon Flip & Spray Bottles. In preparation for WCA measurements, 4 × 4 cm squares of polyester fabric were then sprayed five times each from 6 cm away. Cotton samples were not prepared, as prior work has determined how WCA measurements of similar waxes compare on both polyester and cotton.[12] In preparation for WVP measurements, 9 × 9 cm squares of cotton and polyester fabric were sprayed five times from 6 cm away. All samples were prepared from a single batch of crude and enriched waxes.

For comparison, CommCoat was used to coat the substrates following the manufacturer's instructions. Fabric was cut to similar sizes to those for wax coating. The fabric samples were submerged in RO water and sprayed with CommCoat 20 times from 15 cm away, and the excess was wiped off after 2 min.

All samples were dried using either a General Electric (GE) Electric Compact Dryer (4 cu. ft. model PCVH480EK0WW) on medium heat (ca. 57 °C, timed dry) or Whirlpool dryer (model YWED5620HW1) on medium-high heat (ca. 58 °C, timed dry). Wax samples were dried for 30 min, and CommCoat samples were dried for 60 min. Alternatively, samples were dried overnight in ambient air.

2.3. Characterization Techniques

2.3.1. Moisture Content of Conifer Needles. The moisture content of the needles was measured using a Halogen Moisture Analyzer (Mettler Toledo HC103). A standard drying program was run at 60 °C with switch-off criterion 5 (1 mg/140 s).

2.3.2. Wax Yields. To calculate wax extraction yields, the weights at different stages of purification were measured by using an analytical balance (SECURA324-1S).

2.3.3. Differential Scanning Calorimetry. The thermal properties of waxes were determined using a differential scanning calorimetry (DSC) apparatus (TA Q1000) with 50 mL/min nitrogen flow. 6.0 mg of each sample were[17] loaded into 40 μL aluminum pans, equilibrated at 0 °C for 5 min, then heated by 5 °C/min to 100 °C, cooled to −20 °C, and then reheated to 100 °C.[18] Thermograms were recorded for the first cooling and second heating.

2.3.4. Drying Machine Drum Temperature. The drum temperatures were measured using an infrared radiation (IR) gun (Milwaukee 10:1 Infrared Temp-Gun). Each drying machine was run for a duration of 30 min, with their drum temperature measured every 5 min, and these measurements were averaged. The GE dryer was run on medium heat, and the Whirlpool dryer was run on medium-high heat.

2.3.5. Dynamic Light Scattering (DLS): Dispersion Stability. All plant wax dispersions were vigorously agitated and shaken for about 30 s before being passed through a 0.45 μm syringe filter (Whatman GD/X). A UV−vis spectrophotometer (Shimadzu UV-2600i) was used to capture absorption values. Within 1 day and one month of preparing samples, DLS (Zetasizer Nano-ZS) was used to take three repeat measurements of polydispersity index (PDI), particle size distribution, and Z-average. Using the instrument software, the ζ-potential was calculated, applying the Smoluchowski model.

2.3.6. Water Contact Angle. A tensiometer (Theta Flex 300-Pulsating Drop 200, Attension, Finland) was used to measure static water contact angles (WCAs) at room temperature. Ten microliters of water droplets (purified by Milli-Q) was dispensed onto the coating substrate. Images of the droplet were taken at 1.4 frames/s for 5 min and analyzed using the Laplace−Young fitting mode. Measurements were repeated on at least three locations of one sample for each substrate and coating.

https://doi.org/10.1021/acsaenm.4c00116
ACS Appl. Eng. Mater. 2024, 2, 1288−1297

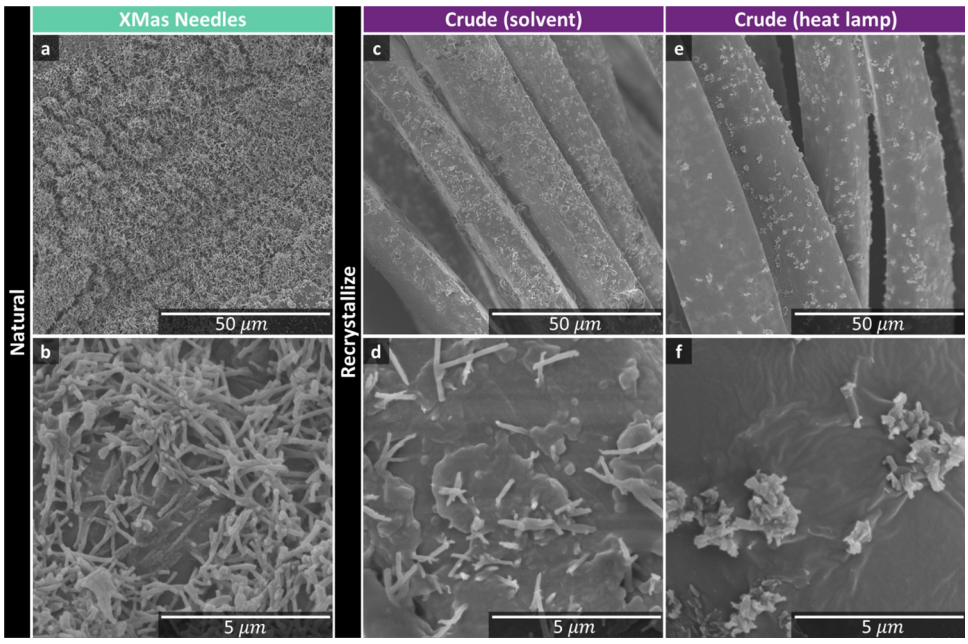

Figure 2. Surface morphologies of natural Christmas (XMas) tree wax compared with crude XMas wax suspensions sprayed onto polyester fabric, air-dried, and recrystallized using various methods. SEM images show crystal density and size decreasing from left to right: (a,b) natural wax on XMas needles, (c,d) solvent recrystallization, and (e,f) heat lamp recrystallization.

2.3.7. Scanning Electron Microscopy. Christmas tree needles were cut into segments, mounted on aluminum stubs using nonconductive double-sided adhesive tape, and sputter coated (Cressington 208HR) with ca. 10 nm of gold. Fabric samples coated with crude wax were mounted on aluminum stubs with glue (Gorilla 100% Tough Epoxy Clear), put under a heat lamp (ca. 58 °C) for 30 min to accelerate curing, and sputter coated with ca. 10 nm of iridium. Conductive liquid silver paint, mixed with acetone to reduce the viscosity, was added to fabric edges, and then, samples were cured under the heat lamp for an additional 30 min. Alternatively, fabric samples coated with crude wax were prepared for scanning electron microscopy (SEM) as before but without the use of a heat lamp to accelerate curing. SEM was carried out in high vacuum (Hitachi S-2600 and SU3500) with a beam spot size of 10, 5 kV accelerating voltage, and a 12 mm working distance.

2.3.8. Water Vapor Permeance. Water vapor permeances (WVPs) were determined gravimetrically (Labthink C360H Water Vapor Transmission Rate Test System, ASTM E96-15 water method) at 25 °C and a relative humidity of 50%, with the coated side of the sample facing the dry side of the apparatus. Sample thicknesses were measured using a digital disc micrometer (Mitutoyo) with 1 μm accuracy.

2.3.9. Qualitative and Quantitative Analyses of Wax Extracts. The composition of laboratory scale, bulk, and fractionated wax extractions of *Abies procera* needles was determined using GC–MS GC–FID, following a procedure similar to Fleetwood et al.[12] The surface areas of the needles were determined using pixel counts of digital images (ImageJ) of flattened needles, assuming negligible needle thickness.[19,20] At the laboratory scale, a known amount of *n*-tetracosane was added to the sample before extraction, and the wax was extracted with chloroform (3 × 20 mL). To prepare the bulk and fractionated extracts for analysis, hot chloroform (ca. 60 °C) was added to each sample until the mixture dissolved completely. A small aliquot (ca. 200 μL) was removed for subsequent analysis.

In preparation for chemical analysis, each sample was dissolved in 20 μL of pyridine and derivatized with 20 μL of BSTFA at 70 °C for 45 min. The derivatized wax compounds were separated by GC (6890N, Agilent). First, an aliquot of sample was injected via a cool-on-column injector into an HP-1 capillary column (Agilent; 30 m length, 320 μm inner diameter, and 0.1 μm film thickness), carried by a 2 mL/min constant flow of hydrogen. The oven was programmed to hold at 50 °C for 2 min, ramp to 200 °C at a rate of 40 °C/min, then hold at 200 °C for 2 min, then ramp to 320 °C at a rate of 3 °C/min, and finally to hold at 320 °C for 30 min. To quantify the wax components, a flame ionization detector (FID, Agilent) with a flame setting of 20 mL/min nitrogen, 30 mL/min hydrogen, and 200 mL/min at 250 °C was used. To identify the wax components, they were separated by GC under the same conditions but with helium as carrier gas at a flow of 1.4 mL/min and a MS detector (5973N, Agilent, Electron impact at 70 eV, m/z 50–800, 1 scan/s).

To determine the chain length and isomer profiles of the secondary alcohols, wax was fractionated by thin-layer chromatography (TLC) on silica plates (1 mm thick, Merck). Bands of compound classes were visualized with UV light (365 nm) after being stained with primuline, scratched from the plates, extracted with chloroform (3 × 20 mL), and derivatized as described above. The resulting samples were analyzed using GC–MS as described earlier, and relative compositions (wt %) of secondary alcohol isomers were determined using the abundance of characteristic fragments.

3. RESULTS AND DISCUSSION

3.1. Christmas Tree Wax Composition

The present study aimed to use XMas trees, collected from tree recycling programs, as a low-value waste source of wax for making a water-repellent spray for coating textiles. Xmas tree waste was anticipated to be an effective source of waxes for this application due to conifer needles' glaucous appearance, often an indicator of hydrophobicity, and high wax loads in our previous work.[12] The XMas trees mostly consisted of noble fir (*Abies procera*).

Here, SEM was used to first investigate the micromorphology of the needle surface. The needles were found to be covered by a dense network of wax nanotubules (Figure 2a,b). This was anticipated, given that similar micromorphologies have been found for other gymnosperm species.[21] Our prior work demonstrated that nanotubule-covered surfaces also showed gymnosperm species to have WCAs in the superhydrophobic range, suggesting that noble fir wax may be well-suited for making water-repellent sprays.[12]

https://doi.org/10.1021/acsaenm.4c00116
ACS Appl. Eng. Mater. 2024, 2, 1288–1297

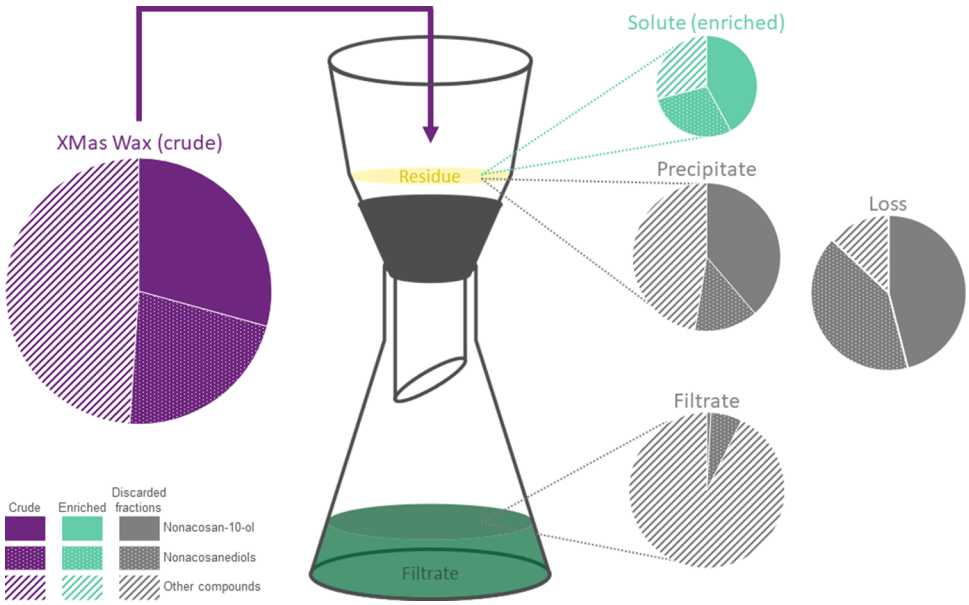

Figure 3. Gas chromatography−mass spectrometry (GC−MS) and gas chromatography−flame ionization detector (GC−FID) were used to determine the composition of the (purple) Christmas (XMas) tree wax extract, (green) residue-solute, (gray) residue-precipitate, filtrate, and loss. For each fraction, the pie chart represents the relative abundance of nonacosan-10-ol (solid), nonacosanediols (dotted), and other compounds (striped, includes triterpenoids, alkyl esters, and unknowns). The area of each pie chart is scaled to the mass recovered for each fraction, relative to the original mass of the crude fraction. The analysis was performed on fractions from two independent purifications with similar results. Both purifications were performed on aliquots from the same crude extract.

To further assess the suitability of noble fir wax for waterproofing sprays, GC−MS and GC−FID analyses were also performed on wax mixtures extracted from detached needles. Approximately 50 μg of wax was found per cm^2 of projected needle surface area, taking only the flat upper and lower sides of the needles into account. However, the true surface area was likely higher due to the finite thickness of the needle, and therefore, the true wax load per surface area was likely slightly less than 50 μg per cm^2.

The noble fir needle wax was composed primarily of secondary alcohols, alkanediols, alkyl esters, and triterpenoids (Figure S1). Small amounts of hydroxyaldehyde (5-hydroxyeicosanal) were also present. The secondary alcohols were largely dominated by nonacosan-10-ol, with only minor amounts (<1%) of heptacosan-10-ol and hentriacontan-10-ol also present. The only alkanediols detected were nonacosanediols. Isomers thereof all had one hydroxyl group on C-10, with the other hydroxyl group found on C-3, C-4, C-5, C-7, or C-13. Notably, over 50% of the mixture consisted of nonacosan-10-ol and nonacosanediols, which are known to cocrystallize and self-assemble into nanotubule crystals when present in high quantities. A broad region of the chromatogram contained various triterpenoids, which combined accounted for almost 20% of the wax mixture (Figure S2). However, triterpenoids, which are amphiphilic polycyclic compounds commonly found in plant wax mixtures, are generally thought to contribute little to leaf surface hydrophobicity.[22]

After the initial analysis confirmed the high wax load and high abundance of tubule-forming compounds in needle waxes of noble fir, large quantities of wax were extracted from waste XMas trees (Figure 1.1−1.3). The resulting wax extract separated into a thin top layer that appeared white and translucent and a thick bottom layer that was green and opaque. The hydrophobicity of both layers was assayed with water drops, showing that the top surface was hydrophobic, while the bottom surface was hydrophilic. These findings suggested that the crude extract contained substantial amounts of hydrophilic components, and we therefore aimed to remove them and thereby increase the concentration of nonacosan-10-ol and nonacosanediols to enhance the crystal formation of the wax and, thus, the performance of its spray application.

3.2. Crude Wax Characterization and Partial Purification

The crude wax, obtained in bulk from XMas trees, had a similar chemical composition to that of the wax extracted on a small scale. The detected compounds included nonacosan-10-ol, nonacosanediols, triterpenoids, alkyl esters, and unidentified compounds. However, the triterpenoids comprised approximately one-third of the mass of the bulk wax yet made up less than 20% of the smaller-scale extract.

Following a simplified procedure modified by McElroy et al., the extract was separated into three components: (1) residue-solute, (2) residue-precipitate, and (3) filtrate. Briefly, the two residue fractions were separated from the filtrate fraction following recrystallization in room-temperature methanol and then separated from each other by decanting from hot methanol. The polarity of each fraction was then qualitatively measured with a drop of water. It was determined that the filtrate fraction was hydrophilic, which is consistent with its solubility in methanol at room temperature. The residue fractions were both hydrophobic, with the residue-solute having a higher WCA.

Chemical analyses with GC−MS and GC−FID were used to analyze the wax compositions of the different wax preparations (Figure 3). The purification process successfully increased the concentration of nanotubule-forming compounds in the residue-solute to 74% (44% nonacosan-10-ol; 30% nonacosanediols). Similarly, the residue-precipitate comprised 46% nanotubule-forming compounds (34% nonacosan-10-ol; 12% nonacosanediols). In contrast, the filtrate had much lower amounts of these compounds, at 9% (1% nonacosan-10-ol; 8%

https://doi.org/10.1021/acsaenm.4c00116
ACS Appl. Eng. Mater. 2024, 2, 1288−1297

nonacosanediols). Because the residue-solute was most enriched in the secondary alcohol and alkanediols, it was chosen as the "enriched" extract.

Comparing the composition and masses of the filtration fractions to those of the crude wax, solubilities of each compound class during the separations can be approximated. In the initial separation, less than 1% of nonacosan-10-ol and about 15% of the nonacosanediols from the crude extract were soluble in room-temperature MeOH, ultimately being recovered as part of the filtrate (Figure 3). However, when the cold-methanol-insoluble (i.e., residue) compounds were placed in hot methanol, only a third of the nonacosan-10-ol went into solution, causing most of the nonacosan-10-ol mass to instead accumulate in the residue-precipitate fraction. About an equal mass of nonacosanediols was found in the hot-methanol-soluble (i.e., residue-solute) and hot-methanol-insoluble (i.e., residue-precipitate) fractions. In all, the percent recovery by mass of nonacosan-10-ol and nonacosanediols in the enriched fraction was 27 and 25%, respectively. Repeating the purification process by recycling and recrystallizing the residue-precipitate and filtrate could result in the recovery of additional nonacosan-10-ol.

The other detected compounds (Figure S3) included diverse triterpenoids, alkyl esters, and unknown compounds. Room-temperature methanol dissolved almost all of the triterpenoids but did not dissolve any detectable amounts of alkyl esters. Upon exposure to hot methanol, the remaining triterpenoids and alkyl esters were unlikely to dissolve. Thus, while the residue-precipitate fraction had more nonacosan-10-ol by mass, the insolubility of the nonpolar triterpenoids and alkyl esters caused the fraction to ultimately have lower relative amounts of nonacosan-10-ol than the residue-solute. The "unknown" compounds showed no clear trend and made up less than 20% of each fraction.

To approximate the behavior of diterpenoid resins overall during the purification process, the most abundant resin acid (dehydroabietic acid DHA) was chosen as a proxy and quantified across the crude wax and the three filtration fractions. From there, the mass ratio of DHA to nonacosan-10-ol was calculated for each fraction. The crude extract contained 0.017 g of DHA/g of nonacosan-10-ol, whereas the enriched extract had only 0.004 g of DHA/g of nonacosan-10-ol, likely indicating a decrease in diterpene resins overall. In contrast, the residue-precipitate contained merely 0.001 g of DHA/g of nonacosan-10-ol, while the filtrate accumulated 3.33 g DHA/g nonacosan-10-ol.

The filtration and all subsequent analyses were performed twice with similar results.

The residue-solute was selected as the "pure" wax extract because it was the most enriched in nonacosan-10-ol compared with the other recovered fractions and the crude extract. However, given that almost 75% of nonacosan-10-ol and nonacosanediols by mass were discarded or lost during the purification process, it is important to look at the performance of the coating to determine whether the purification process is necessary. Purification additionally requires more time and expense and adds environmental hazards and waste to the production process. Therefore, we will compare the coating performance between the crude and enriched conifer wax throughout the remainder of the results and discussion.

3.3. Conifer Wax Dispersion Stability with Time

Aqueous plant wax particle dispersions containing 0.01 g/mL XMas tree wax were made with no additional stabilizers and emulsifiers. Visually, there was minimal sedimentation observed over a three-month period, as shown in Figure 1h. Prior to characterizing the dispersions, they were shaken vigorously, similar to what is instructed on the labeling for commercially available coatings. After shaking, no sediment was visible.

DLS was used to characterize dispersions of both crude and enriched wax mixtures. In all cases, the size distribution was sufficiently narrow for DLS measurements as the PDI was less than 0.7. The same-day samples had ζ-potentials of -67.2 ± 0.9 mV for crude dispersions and -78.3 ± 1.8 mV for enriched dispersions (Table 1). Therefore, the net negative surface charges of these wax particles demonstrated excellent stability behavior without the propensity to flocculate or coagulate.[23]

Table 1. Average (3 Runs Each) Z-avg, PDI, and ζ-Potential of Plant Wax Dispersions Using 0.01 g/mL Aqueous Wax Dispersions from XMas Trees[a]

material	Z-avg (nm)	PDI	ζ-potential (mV)	time
crude	188 ± 1	0.101 ± 0.017	−67.2 ± 0.9	1 day
crude	199 ± 1	0.110 ± 0.018	−55.7 ± 1.6	1 month
enriched	193 ± 2	0.143 ± 0.012	−78.3 ± 1.8	1 day
enriched	192 ± 3	0.122 ± 0.021	−61.3 ± 0.4	1 month

[a]Time is after dispersion preparation.

Lozhechnikova et al. attributed this high electrostatic charge source to the amphiphilic character of wax compounds.[24] Therefore, we theorized that upon heating and dispersing the amphiphilic wax molecules, they melted, allowing them to become more mobile and self-assembled into micelles. We believe that this molecular arrangement of a hydrophilic outer layer and hydrophobic core is what gives the dispersion its stability.

DLS was also used to assess the stability of the plant wax dispersions with storage time. Immediately after making the dispersions and after 1 month of storage, the Z-average (Z-avg) increased from 188 ± 1 nm (PDI = 0.101) to 199 ± 1 nm (PDI = 0.110) for crude wax and decreased from 193 ± 2 nm (PDI = 0.143) to 192 ± 3 nm (PDI = 0.122) for enriched wax (Table 1). After 1 month, ζ-potentials were -55.7 ± 1.6 mV for crude dispersions and -61.3 ± 0.4 mV for enriched dispersions. The intensity distributions show how particles are dispersed within a medium, indicating whether they are uniformly dispersed (stable) or clumped together (unstable). With respect to time, if the intensity distribution changes, this suggests instability within the dispersion. Over the 1 month period, the slight changes in particle size, combined with low and relatively stable PDIs and ζ-potentials greater than 40, suggest that the dispersions maintained good or excellent stability over time. Furthermore, these systems exhibited reasonable homogeneity in particle size with PDIs near 0.1.[23] Stability was further evident by the intensity distributions, which were essentially indistinguishable from one another (Figure S4). The stability of plant wax dispersions containing no emulsifiers over time is consistent with previous work.[12]

3.4. Surface Morphology of Wax-Coated Samples

To attain superhydrophobicity, both hierarchical surface roughness and low surface energy are needed, with the former

https://doi.org/10.1021/acsaenm.4c00116
ACS Appl. Eng. Mater. 2024, 2, 1288−1297

being the focus of this section and the latter the focus of the next section.[5,6] In this study, hierarchical surface roughness was attributed to two main factors: the inherent roughness of the textile's texture and the microroughness imparted by the applied coating. Comparing the textiles, it was qualitatively observed that the substrate surface roughness increased, moving from the rain jacket to polyester and being the greatest with cotton.

In the case of the coating, nonacosan-10-ol and nonacosanediols recrystallized into wax tubules by using different methods. DSC measurements were conducted to determine the ideal temperatures for the melting and subsequent recrystallization of plant waxes (Figure 4). Complete melting

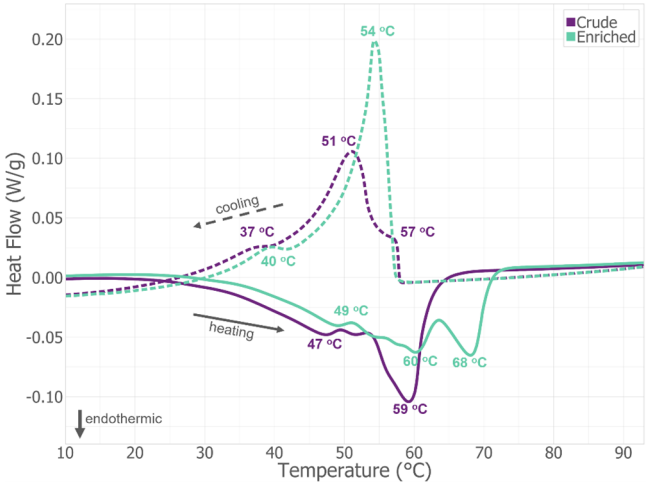

Figure 4. Melting behavior of enriched (green) and crude (purple) Christmas tree wax determined by DSC. For crude wax, complete melting occurred at approximately 59 °C, and a heat absorption peak was present at roughly 47 °C. For enriched wax, complete melting occurred at 68 °C, and heat absorption peaks were present at approximately 49 and 60 °C. Endothermic is down.

of crude and enriched XMas tree wax occurred at approximately 59 and 68 °C, respectively. Additionally, a single heat absorption peak was present for crude wax at roughly 47 °C, while enriched wax had two peaks at approximately 49 and 60 °C. Based on these DSC measurements, the ideal temperature for annealing fabric samples was between approximately 47 and 59 °C for the crude coating and 49−60 °C for the enriched coating.

These results were in line with literature values for pure nonacosan-10-ol, in which complete melting occurred at 75 °C and a solid−liquid transition occurred at 54 °C. Here, exothermic peaks appeared at 68 and 50.5 °C.[13] This shift to slightly lower temperatures is likely due to the impurities present in both the crude and enriched samples.

Considering that users have access to home drying machines for heat treatment, we evaluated whether these machines could reach the annealing temperatures needed. The drying machine drum temperatures were measured to be 57.2 °C for GE and 58.5 °C for Whirlpool, both falling within the range established by our DSC data for recrystallization.[10]

SEM was used to investigate the surface morphology and extent of the wax coatings and thereby assess changes in crystalline morphology upon heat treating. Uncoated polyester fabric, along with the rain jacket material and commercially coated polyester fabric, appeared smooth with no obvious structure present. When the polyester fabric was sprayed with XMas tree wax coatings and left to air-dry, without a heat treatment process applied, the coatings appeared as spherical particles (Figure 5g−j). Upon heating, these coatings are assembled into tubules in the home drying machine (Figure 5k−n) or after being placed under a heat lamp (Figure 2e,f). In a comparison of the efficacy of the recrystallization techniques, natural XMas tree wax yielded (Figure 2a,b) the largest crystal numbers and sizes, followed by solvent evaporation (Figure 2c,d), heating in the home drying machine (Figure 5k−n), and the heat lamp being the least effective (Figure 2e,f). Furthermore, the enriched wax coating (Figure 5k,l) had a greater density of tubular crystals in comparison to the crude wax coating (Figure 5m,n).

Comparing the crystal density of natural XMas wax to heat-treated wax, it is speculated that only partial melting is occurring and that this is because the temperature settings used on the drying machine were just below the melting points of the crude and enriched XMas tree wax. Therefore, it is theorized that some of the wax is melting and spreading across the surface while also allowing for molecular rearrangement into a tubular structure. Thus, the coating's coverage across the substrate was improved, while the crystals' surface-to-volume ratios were increased. These findings agreed with Matas et al.'s results.[13]

In summary, comparing these heat treatment methods to naturally occurring wax found on XMas tree needles (Figure 2a,b), the home drying machine gave the most similar wax morphology, consisting of tubular structures. Moreover, both solvent evaporation and annealing enabled the mobility of wax molecules, allowing them to self-assemble into the characteristic tubular crystals.[24] So far, a surface roughness increased by the coating of the enriched and crude coatings has been qualitatively verified using SEM. Furthermore, this tubular structure suggests the presence of nonacosan-10-ol, which has been further verified using GC−MS. Therefore, a nonpolar surface chemistry is likely present. Both high surface roughness and a nonpolar chemistry are essential properties for achieving superhydrophobicity. In the next section, superhydrophobicity will be further verified quantitatively using WCA measurements, also in context with the breathability of the samples.

3.5. Hydrophobicity and Breathability Performance of Wax Coatings

Water repellency and breathability are often opposing properties in lightweight material coatings. Specifically, thicker coatings may increase the WCA but also effectively seal the fabric and impede WVP.[10] Therefore, WCA and WVP were compared for a trilaminate rain jacket material, uncoated polyester fabric, and polyester fabric that was either coated using a commercial product or coated with conifer wax dispersions containing different amounts of nonacosan-10-ol and alkanediols. The method of drying the conifer wax coating was also compared and included heat from a home drying machine or air drying.

In prior work, it had been observed that WCA increased with increasing surface roughness, and therefore, it was assumed that changing the substrate surface would have similar results here.[12] Additionally, Jetter et al. concluded that the substrate's surface polarity did not influence recrystallization.[25] Therefore, only the WCA of polyester samples were measured, as these have a lower error in WCA measurements than cotton samples. However, given that WVP was not

https://doi.org/10.1021/acsaenm.4c00116
ACS Appl. Eng. Mater. 2024, 2, 1288−1297

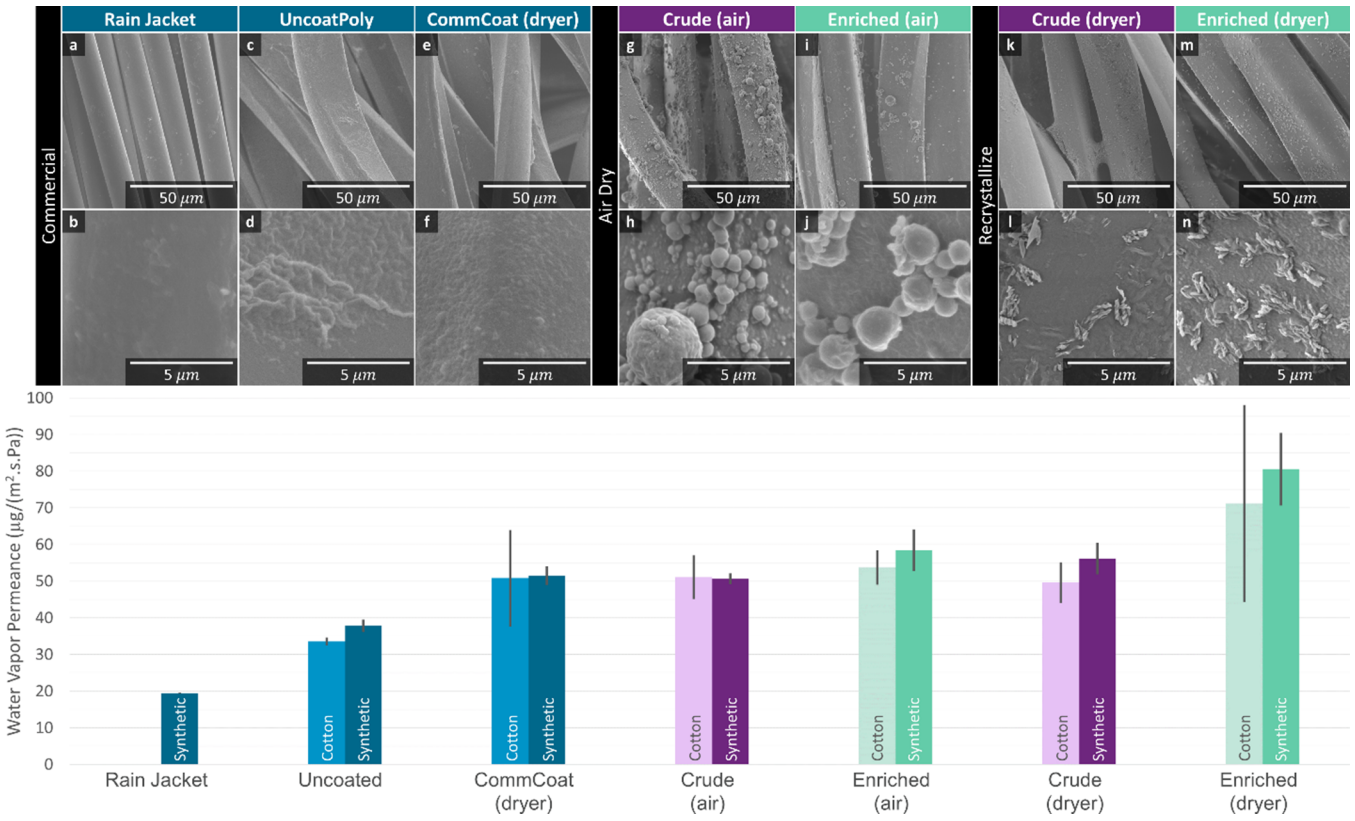

Figure 5. SEM images of enriched (green: i and j, m and n) and crude (purple: g and h, k and l) Christmas (XMas) tree wax sprayed polyester textiles, which were then dried in a home drying machine (dryer: k and n) or air-dried (air: g–j). XMas tree wax coatings (green and purple: g–n) are compared with synthetic materials (blue: a–f), including PFC-free coated rain jacket material (a and b), uncoated polyester (c and d), and a commercial coating (e and f). Water vapor permeability measurements are shown for all of the SEM samples (synthetic) as well as cotton-coated textiles (cotton).

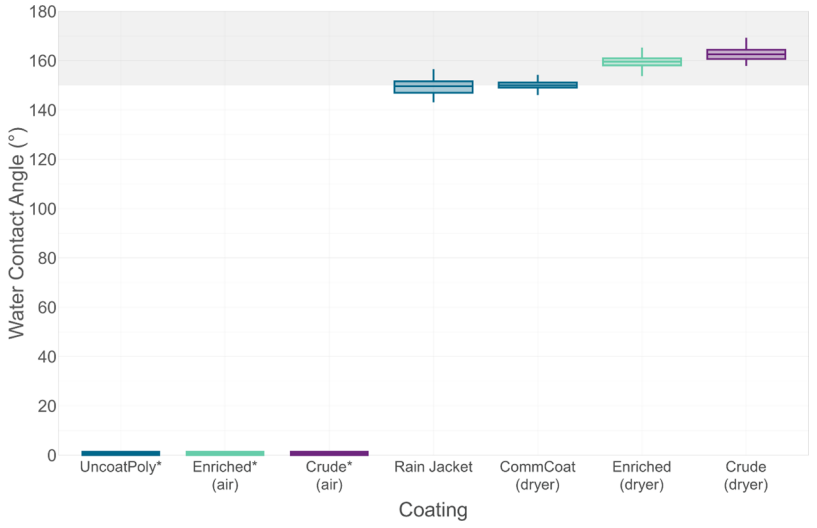

Figure 6. Static WCA measurements of enriched (green) and crude (purple) Christmas (Xmas) tree wax sprayed onto polyester textiles and dried in a home drying machine (dryer) or air-dried (air). XMas tree wax coatings are compared to synthetic materials (blue), including uncoated polyester, PFC-free coated rain jacket material, and a commercial coating. *Wetting was nearly instantaneous and unmeasurable for uncoated polyester, along with air-dried enriched and crude XMas tree wax-coated polyester. The gray box indicates the superhydrophobic WCA range.

measured in previous work, both cotton and polyester samples were tested for breathability.

WCAs were 149.5 ± 2.6° for the rain jacket, 150 ± 2.6° for commercially coated polyester fabric, 159.0 ± 6.6° for enriched home-dried polyester, and 162.7 ± 2.6° for crude home-dried polyester (Figure 6). The remaining samples were wetted almost instantaneously and had unmeasurable WCAs, including the uncoated polyester, the air-dried coating with enriched wax, and the air-dried coating with crude wax. The crude conifer wax spray gave coatings with a similar but slightly higher hydrophobicity compared with those from the purified conifer wax spray when dried in a home drying machine. Both

https://doi.org/10.1021/acsaenm.4c00116
ACS Appl. Eng. Mater. 2024, 2, 1288–1297

were more hydrophobic than the rain jacket and the commercial coating. Uncoated polyester and air-dried samples were wetted in under 5 min. When not heat treating the air-dried samples, melting and recrystallization could occur, resulting in a lack of coating coverage and tubule formation, as observed in the SEM images.[12] Additionally, given that the coating is prepared as an aqueous dispersion, it is surmised that the midchain polar hydroxyl groups are exposed, coming in contact with the water droplet, and nonpolar methyl groups are buried within the spherical particle that the coating forms when sprayed onto substrates (Figure 5g–j).[26] This was consistent with previous findings by Fleetwood et al.[12]

After the surface polarities were determined, samples were subjected to WVP experiments to assess their breathabilities. WVPs were 19.4 ± 0.2 $\mu g/m^2 \cdot s \cdot Pa$ for the rain jacket, 33.6 ± 1.1 and 37.9 ± 1.7 $\mu g/m^2 \cdot s \cdot Pa$ for uncoated cotton and polyester, 50.8 ± 13.1 and 51.5 ± 2.5 $\mu g/m^2 \cdot s \cdot Pa$ for commercially coated home-dried polyester, 53.8 ± 4.6 and 58.5 ± 5.7 $\mu g/m^2 \cdot s \cdot Pa$ for enriched wax air-dried on cotton and polyester, 49.6 ± 5.6 and 56.2 ± 4.3 $\mu g/m^2 \cdot s \cdot Pa$ for crude wax home-dried on cotton and polyester, and 71.2 ± 26.9 and 80.6 ± 9.9 $\mu g/m^2 \cdot s \cdot Pa$ for enriched wax home-dried on cotton and polyester (Figure 5). The rain jacket material had the lowest breathability, followed by uncoated cotton and then polyester (synthetic). The WVPs of textiles that were coated with a commercial coating (drying machine), crude wax coating (air-dried), enriched wax coating (air-dried), and crude wax coating (drying machine) were all fairly similar. However, the enriched wax coating (drying machine) showed the highest breathability. It seems plausible that this is due to a more uniform coating of the surface than on the air-dried samples, as shown in the SEM images. The difference between pure wax-dryer vs crude wax-dryer coatings may be due to pores between fibers being filled with polar compounds such as resins, resulting in both smaller and fewer pores between fibers.

4. CONCLUSIONS

Hydrophobic coatings prepared from aqueous plant wax dispersions that are free of PFCs and petroleum were developed through homogenization without the use of stabilizers or surfactants. For this, wax from plant waste streams was utilized, with a focus shifting from deciduous sources in prior work to conifer sources in the current work in order to improve the circularity of the process by using a low-value waste stream produced within the industry.[12] The dispersions were subsequently applied to textiles through spraying and then heat-treated using home drying machines. This method mirrors the application process of commercial coatings, which consumers can easily apply at home.

The crude and enriched conifer wax coatings were then tested for their dispersion stability, hydrophobicity, and breathability. All of the dispersions prepared had good to excellent stability and reasonable particle size homogeneity. In comparing crude vs enriched XMas wax coatings, the enriched coating had a greater WVP, while the crude coating was more hydrophobic. However, both the enriched and crude conifer wax coatings were more hydrophobic and breathable than those of commercial products.

Considering that the hydrophobicities of crude wax-dryer and pure wax-dryer coatings were very similar, selecting a coating comes down to breathability and economic decisions. In applications where high breathability is crucial, the pure wax-dryer coating would be worth applying. However, given that the breathability of both the pure wax-dryer and crude wax-dryer was greater than that of the commercial coatings, in most applications, the crude wax-dryer coating would be the better choice, given the cost savings and reduced environmental impact gained from not losing extract during the purification process. Additionally, the crude wax-heat coating may be more durable due to the increased adhesion that the sap may provide, given its ductility between the textile and the wax, which is more brittle. Contradictory to our initial hypothesis that purifying the wax extract is essential to the performance, it was concluded that the differences in performance between the enriched and crude coatings were minor, in comparison to the economic and environmental benefits of the reduced number of purification steps in producing the crude coating. In summary, we created a water-repellent spray using crude XMas tree extracts that can be easily applied at home by users. This spray is not only more environmentally friendly compared to existing products on the market but also has superior performance.

In future work, we plan to test the wash-cycle durability to further verify whether the performance of the crude and enriched coatings is affected. Additionally, conducting toxicity testing in future work is of interest. While the needle extracts of various conifer plant species are consumed in a number of beverages ranging from tea to alcohol,[27] toxicity testing would need to be carried out in order to see if when concentrated these wax extracts have any impact on human health.

Additionally, one potential limitation of sourcing tubule-forming waxes from XMas trees is the seasonal availability of this source and its broad geographic distribution post holidays, which may pose challenges for commercial scalability. However, it is believed that this purification process can be more broadly applied to a number of other conifer species. An alternative source to XMas trees could be slashed piles, which offer a large and nonseasonable supply of conifer trees in a localized area. Future studies should therefore consider evaluating the efficacy of this purification process using conifer needles sourced from slash piles.

■ ASSOCIATED CONTENT

Supporting Information

The Supporting Information is available free of charge at https://pubs.acs.org/doi/10.1021/acsaenm.4c00116.

Lab-scale analysis of noble fir (*Abies procera*) needle wax (Figure S1), gas chromatography–mass spectrometry total ion intensity vs elution time for TMS-derivatized noble fir wax extract (Figure S2), sequential separations of the wax mixture using methanol to identify compound class compositions (Figure S3), and dynamic light scattering of purified and impurified Christmas tree wax dispersions (Figure S4) (PDF)

■ AUTHOR INFORMATION

Corresponding Author

E. Johan Foster − *Department of Chemical and Biological Engineering 421, University of British Columbia, Vancouver, BC V6T 1Z3, Canada;* orcid.org/0000-0002-4103-8510; Email: johan.foster@ubc.ca

https://doi.org/10.1021/acsaenm.4c00116
ACS Appl. Eng. Mater. 2024, 2, 1288−1297

Authors

Sara K. Fleetwood − *Department of Chemical and Biological Engineering 421, University of British Columbia, Vancouver, BC V6T 1Z3, Canada;* orcid.org/0000-0001-9692-6833

Sydney Bell − *Department of Chemistry, University of British Columbia, Vancouver, BC V6T 1Z1, Canada;* orcid.org/0009-0000-3776-7668

Reinhard Jetter − *Department of Chemistry, University of British Columbia, Vancouver, BC V6T 1Z1, Canada; Department of Botany, University of British Columbia, Vancouver, BC V6T 1Z4, Canada*

Complete contact information is available at: https://pubs.acs.org/10.1021/acsaenm.4c00116

Author Contributions

The manuscript was written through contributions of all authors. All authors have given approval to the final version of the manuscript.

Funding

The authors gratefully acknowledge the financial support provided by the NSERC Canfor Industrial Research Chair in Advanced Bioproducts (# 553449-19), NSERC Discovery Grant (RGPIN-2021-03172), the Canada Foundation for Innovation (Project number 022176), the Pacific Economic Development Canada (PacifiCan), and Natural Sciences and Engineering Research Council (Canada) Discovery Grants Program (grant #262461).

Notes

The authors declare no competing financial interest.

■ ACKNOWLEDGMENTS

The authors gratefully acknowledge the financial support provided by the NSERC Canfor Industrial Research Chair in Advanced Bioproducts, (# 553449-19), NSERC Discovery Grant (RGPIN-2021-03172), the Canada Foundation for Innovation (Project number 022176), the Pacific Economic Development Canada (PacifiCan), and Natural Sciences and Engineering Research Council (Canada) Discovery Grants Program (grant #262461). The authors would also like to thank the UBC Bioimaging facility (RRID: SCR021304) for their technical assistance and use of their facilities.

■ REFERENCES

(1) Kumar, A. *Hydrophobic and Superhydrophobic Coatings: Technologies and Global Markets*. Wellesley, 2016.

(2) Oliver, J. *Bioinspired and Nanoengineered Surfaces: Technologies*; Applications and Global Markets: Wellesley, 2018.

(3) Schellenberger, S.; Hill, P. J.; Levenstam, O.; Gillgard, P.; Cousins, I. T.; Taylor, M.; Blackburn, R. S. Highly fluorinated chemicals in functional textiles can be replaced by re-evaluating liquid repellency and end-user requirements. *J. Clean Prod* **2019**, *217*, 134−143.

(4) Ensikat, H. J.; Ditsche-kuru, P.; Neinhuis, C.; Barthlott, W. Superhydrophobicity in perfection: the outstanding properties of the lotus leaf. *Beilstein Journal of Nanotechnology* **2011**, *2*, 152−161.

(5) Gorb, S. *Functional Surfaces in Biology: Little Structures with Big Effects*. Vol. *1*. Springer; 2009.

(6) Wang, W.; Lockwood, K.; Boyd, L. M.; Davidson, M. D.; Movafaghi, S.; Vahabi, H.; Khetani, S. R.; Kota, A. K. Superhydrophobic Coatings with Edible Materials. *ACS Appl. Mater. Interfaces* **2016**, *8*, 18664−18668.

(7) Som, C.; Wick, P.; Krug, H.; Nowack, B. Environmental and health effects of nanomaterials in nanotextiles and façade coatings. *Environ. Int.* **2011**, *37*, 1131−1142.

(8) Bayer, I. S.; Fragouli, D.; Martorana, P. J.; Martiradonna, L.; Cingolani, R.; Athanassiou, A. Solvent resistant superhydrophobic films from self-emulsifying carnauba wax−alcohol emulsions. *Soft Matter* **2011**, *7*, 7939−7943.

(9) Forsman, N.; Lozhechnikova, A.; Khakalo, A.; Johansson, L.-S.; Vartiainen, J.; Österberg, M. Layer-by-layer assembled hydrophobic coatings for cellulose nanofibril films and textiles, made of polylysine and natural wax particles. *Carbohydr. Polym.* **2017**, *173*, 392−402.

(10) Forsman, N.; Johansson, L.-S.; Koivula, H.; Tuure, M.; Kääriäinen, P.; Österberg, M. Open coating with natural wax particles enables scalable, non-toxic hydrophobation of cellulose-based textiles. *Carbohydr. Polym.* **2020**, *227*, No. 115363.

(11) Barthlott, W.; Neinhuis, C. Purity of the sacred lotus, or escape from contamination in biological surfaces. *Planta* **1997**, *202*, 1−8.

(12) Fleetwood, S. K.; Bell, S.; Jetter, R.; Foster, E. J. Plant-based, aqueous, water-repellent sprays for coating textiles. *Soft Matter* **2023**, *19*, 7020−7032.

(13) Matas, A. J.; Sanz, M. J.; Heredia, A. Studies on the structure of the plant wax nonacosan-10-ol, the main component of epicuticular wax conifers. *Int. J. Biol. Macromol.* **2003**, *33*, 31−35.

(14) Chastagner, G. A.; Riley, K. L. Postharvest Quality of Noble and Nordmann Fir Christmas Trees. *HortScience HortSci.* **2003**, *38*, 419−421.

(15) Riederer, M. *The Cuticles of Conifers: Structure, Composition and Transport Properties*. In: Schulze, E.-D.; Lange, O. L.; Oren, R., editors. Forest Decline and Air Pollution, Springer Berlin Heidelberg: Berlin, Heidelberg, 1989; p 157−192.

(16) Mcelroy, C. R.; Attard, T. M.; Farmer, T. J.; Gaczynski, A.; Thornthwaite, D.; Clark, J. H.; Hunt, A. J. Valorization of spruce needle waste via supercritical extraction of waxes and facile isolation of nonacosan-10-ol. *J. Clean Prod* **2018**, *171*, 557−566.

(17) Gaillard, Y.; Mija, A.; Burr, A.; Darque-ceretti, E.; Felder, E.; Sbirrazzuoli, N. Green material composites from renewable resources: Polymorphic transitions and phase diagram of beeswax/rosin resin. *Thermochim. Acta* **2011**, *521*, 90−97.

(18) Zhang, W.; Lu, P.; Qian, L.; Xiao, H. Fabrication of superhydrophobic paper surface via wax mixture coating. *Chemical Engineering Journal* **2014**, *250*, 431−436.

(19) Abramoff, M.; Magalhães, P.; Ram, S. J. Image Processing with ImageJ. *Biophotonics Int.* **2003**, *11*, 36−42.

(20) Wen, M.; Buschhaus, C.; Jetter, R. Nanotubules on plant surfaces: Chemical composition of epicuticular wax crystals on needles of Taxus baccata L. *Phytochemistry* **2006**, *67*, 1808−1817.

(21) Jetter, R; Kunst, L; Samuels, A. L.. *Composition of Plant Cuticular Waxes*. In Annual Plant Reviews Vol. 23: Biology of the Plant Cuticle, 2006; p 145−181. DOI: 10.1002/9780470988718.ch4.

(22) Seufert, P.; Staiger, S.; Arand, K.; Bueno, A.; Burghardt, M.; Riederer, M. Building a Barrier: The Influence of Different Wax Fractions on the Water Transpiration Barrier of Leaf Cuticles. Front. *Plant Sci.* **2022**, *12*, 12.

(23) Hunter, R. J. *Zeta Potential in Colloid Science: Principles and Applications*. Academic Press: London, New York, 1981.

(24) Lozhechnikova, A.; Bellanger, H.; Michen, B.; Burgert, I.; Österberg, M. Surfactant-free carnauba wax dispersion and its use for layer-by-layer assembled protective surface coatings on wood. *Appl. Surf. Sci.* **2017**, *396*, 1273−1281.

(25) Jetter, R.; Riederer, M. In vitro Reconstitution of Epicuticular Wax Crystals: Formation of Tubular Aggregates by Long-Chain Secondary Alkanediols. *Botanica Acta* **1995**, *108*, 111−120.

(26) Holloway, P. J.; Jeffree, C. E.; Baker, E. A. Structural determination of secondary alcohols from plant epicuticular waxes. *Phytochemistry* **1976**, *15*, 1768−1770.

(27) Kim, K.-Y.; Chung, H.-J. Flavor Compounds of Pine Sprout Tea and Pine Needle Tea. *J. Agric. Food Chem.* **2000**, *48*, 1269−1272.